Chinese Chemical Letters 36 (2025) 110084

Contents lists available at ScienceDirect

Chinese Chemical Letters

journal homepage: www.elsevier.com/locate/cclet

Apatinib potentiates doxorubicin with cRGD-functionalized pH-sensitive micelles against glioma

Hongyi Huang[a,1], Siyao Che[a,1], Wenjie Zhou[b,c,1], Yunchu Zhang[a], Weiling Zhuo[a], Xijing Yang[d], Songping Zheng[a,*], Jiagang Liu[a,*], Xiang Gao[a,*]

[a] Department of Neurosurgery and Institute of Neurosurgery, State Key Laboratory of Biotherapy, West China Hospital, West China Medical School, Sichuan University, Chengdu 610041, China
[b] Department of Laboratory Medicine, West China Second University Hospital, Sichuan University, Chengdu 610041, China
[c] Key Laboratory of Birth Defects and Related Diseases of Women and Children (Sichuan University), Ministry of Education, Chengdu 610041, China
[d] The Experimental Animal Center of West China Hospital Sichuan University, Chengdu 610041, China

ARTICLE INFO

Article history:
Received 26 February 2024
Revised 30 May 2024
Accepted 3 June 2024
Available online 4 June 2024

Keywords:
Apatinib
Doxorubicin
Glioma
Nanomicelle
Co-delivery

ABSTRACT

Glioma is a severe malignant brain tumor marked by an exceedingly dire prognosis and elevated incidence of recurrence. The resilience of such tumors to chemotherapeutic agents, coupled with the formidable obstacle the blood-brain barrier (BBB) presents to most pharmacological interventions are major challenges in anti-glioma therapy. In an endeavor to surmount these impediments, we have synergized pH-sensitive nanoparticles carrying doxorubicin and apatinib to amplify the anti-neoplastic efficacy with cyclic arginine–glycine–aspartate acid (cRGD) modification. In this study, we found that the combination of doxorubicin (DOX) and apatinib (AP) showed a significant synergistic effect, achieved through cytotoxicity and induction of apoptosis, which might be due to the increased intracellular uptake of DOX following AP treatment. Besides, polycaprolactone-polyethylene glycol-cRGD (PCL-PEG-cRGD) drug carrier could cross the BBB by its targeting ability, and then deliver the drug to the glioma site *via* pH-responsive release, increasing the concentration of the drugs in the tumor. Meanwhile, DOX/AP-loaded PCL-PEG-cRGD nanoparticles effectively inhibited cell proliferation, enhanced glioma cell apoptosis, and retarded tumor growth *in vivo*. These results collectively identified DOX/AP-loaded PCL-PEG-cRGD nanoparticles as a promising therapeutic candidate for the treatment of glioma.

Glioma is a common primary malignant tumor of the central nervous system (CNS) that originates from CNS glial cells and accounts for 81% of all CNS tumors, associated with extremely poor survival [1]. The current standard treatment of glioma is maximal safe surgical resection, followed by radiotherapy and temozolomide (TMZ) therapy, yet, the efficacy of recent treatment is limited compared to other cancers [2]. A major reason is the existence of the blood-brain barrier (BBB), which causes insufficient drug concentrations in tumor [3]. Doxorubicin (DOX) is a widely used chemotherapeutic agent with broad-spectrum activities against solid tumors [4,5]. Certainly, accumulating evidences have demonstrated the efficacy of DOX against primary glioma [5,6]. DOX inhibits tumor proliferation through two mechanisms (i) intercalating into DNA and inhibiting topoisomerase II-mediated DNA replication (ii) entering mitochondria to form a semiquinone radical to trigger apoptosis pathway [7]. However, the use of DOX is accompanied adverse effects, including fatal cardiotoxicity and dose-limiting myelosuppression [8,9]. Moreover, similar to other broad-spectrum chemotherapeutic drugs, DOX often encounters the challenge of developing drug resistance in the later stage, increasement of dosage will lead to severe side effects.

In addition to malignant proliferation, the progression of tumor heavily depends on blood vessel formation, which provides nutrition to tumor and maintain immunosuppressive microenvironment. The vascular endothelial growth factor protein family (VEGF) is a powerful regulator of vascular development and is typically implicated in tumor angiogenesis [10]. Studies show that VEGF is overexpressed in various head and neck tumor tissues, with particular in glioma [11]. In most cases, the overexpression of VEGF indicates larger tumor size and a pronounced remodeling of the vascular structure in glioma [12]. As a tyrosine kinase inhibitor, apatinib (AP) selectively inhibits VEGF receptor 2 (VEGFR-2) leading to inducing apoptosis and reversing drug resistance [13]. Furthermore,

* Corresponding authors.
E-mail addresses: zhengsongping2022@163.com (S. Zheng), jiagang_liu@163.com (J. Liu), xianggao@scu.edu.cn (X. Gao).
[1] These authors contributed equally to this work.

https://doi.org/10.1016/j.cclet.2024.110084
1001-8417/

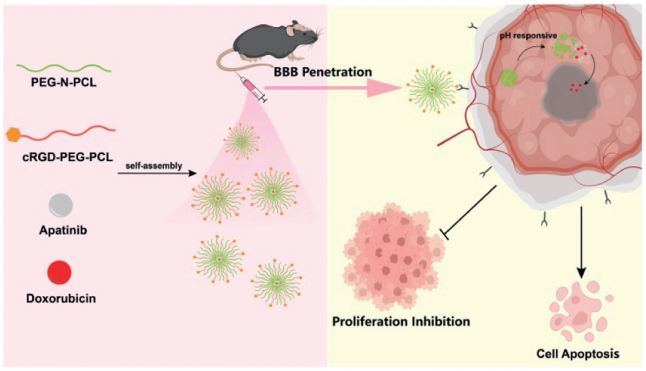

Scheme 1. Schematic illustration of the system of co-loading DOX and AP by pH-sensitive PCL-PEG-cRGD nanoparticles. The cRGD/PEG-N-PCL@DOX + AP micelles were prepared through self-assembly using PEG-N-PCL, cRGD-PEG-PCL, AP, and DOX. Subsequently, the drug effectively accumulated in the tumor site through the targeting and pH-responsive properties of the carrier, resulting in the synergistic anti-tumor effects of AP and DOX.

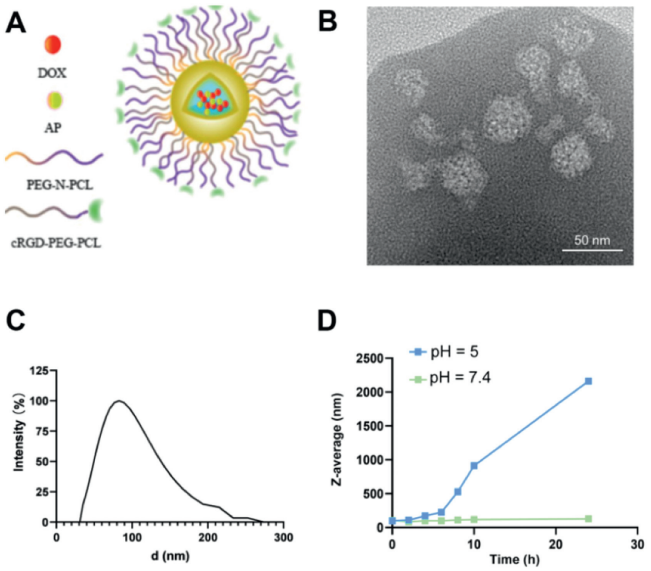

Fig. 1. Characteristics of cRGD/PEG-N-PCL@DOX + AP micelles. (A) Schematic diagram of cRGD/PEG-N-PCL@DOX + AP micelles. (B) TEM image of cRGD/PEG-N-PCL@DOX + AP micelles. (C) Particle size of cRGD/PEG-N-PCL @DOX + AP micelles. (D) pH sensitivity measurement of cRGD/PEG-N-PCL @DOX + AP micelles.

AP has displayed promising therapeutic outcomes in both preclinical research and clinical trials for glioma [14,15]. Taken together, it will be of great interest to combine DOX with AP in glioma treatment.

However, the poor bioavailability of AP and DOX as hydrophobic drugs, and the low permeability to the BBB, collectively limit their therapeutic application in brain tumors. Nano-based drug delivery systems (NDDS) are expected to overcome the shortcomings. Nanoparticles have different sizes, shapes, materials and biological activities, which are ideal drug delivery systems with many advantages including increasing drug water solubility, improving bioavailability and reducing systemic toxicity [16–20]. In addition, through targeted modification of nanoparticles and structure reconstruction for conditional responsiveness, drugs can also be selectively anchored and delivered to the tumor site, thereby achieving therapeutic dose windows. Polyethylene glycol-poly(ε-caprolactone) copolymer (PEG-PCL) is a nanocopolymer based on hydrophilic PEG and hydrophobic PCL, which is highly biocompatible and biodegradable, and widely used in the development of NDDS [21]. Integrin $\alpha v\beta 3$ is highly expressed on the surface of some tumor cells, while its expression is limited or even absent in normal tissues. Integrin-targeting arginine–glycine–aspartate acid (RGD) peptides have been used to enhance the tumor-targeting ability of copolymer nanoparticles for the treatment of a variety of malignancies [22–24], and cyclic RGD (cRGD) is superior to linear RGD peptides based on its resistance to proteolysis and conformational restriction [25]. Moreover, taking advantage of the inherent differences between tumor microenvironment and normal tissues, the pH-sensitive drug delivery system has become an ideal choice for targeted and controlled release [26,27]. In our study, we modified PEG-PCL with cRGD peptide to obtain cRGD-PEG-PCL and designed PEG-N-PCL by introducing imine bonds in PEG-PCL to obtain pH-sensitive nanoparticles, endowing the fabricated nanoparticles with tumor targeting-capability and tumor microenvironment responsiveness (Scheme 1).

In general, a pH-responsive and tumor targeted nanoparticle was prepared in this study for co-delivery of DOX and AP to enhance the BBB penetration and tumor targeting ability of both drugs against glioma. Scheme 1 shows the self-synthesized tumor-targeting nanoparticles loaded with DOX and AP cross the BBB to reach the tumor site, and exhibits synergistic anti-tumor effects in glioma therapy. The therapeutic efficacy on glioma was evaluated both *in vitro* and *in vivo*. In addition, the underlying anti-tumor mechanism and biosafety of this nanoparticle have also been investigated. Finally, the results suggest that simultaneous delivery of DOX and AP by pH-sensitive and tumor targeting nanoparticles can significantly improve the anti-tumor effect, which has a broad application prospect in the treatment of glioma.

First of all, the synthesis of PEG-N-PCL was introduced in Fig. S1 (Supporting information), and chemical structure of PCL-CHO (Fig. S2 in Supporting information) and PEG-N-PCL (Fig. S3 in Supporting information) were verified by ^{1}H NMR. Similarly, the preparation of PCL-PEG-cRGD was listed in Fig. S4 (Supporting information), and chemical structure of maleimide-poly(ethylene glycol)-poly(lactide) (MAL-PEG-PCL) (Fig. S5 in Supporting information) and PEG-PCL-cRGD (Fig. S6 in Supporting information) were verified by ^{1}H NMR. In addition, the structure of PEG-N-PCL and MAL-PEG-PCL were also verified by gel permeation chromatography (GPC), which showed good monodispersity (Figs. S7A and B in Supporting information). The cRGD/PEG-N-PCL@DOX + AP complex was synthesized by self-assembly way for co-encapsulation of DOX and AP, which was prepared by ultrasonication and film dispersion. The core-shell structure of cRGD/PEG-N-PCL@DOX + AP was introduced in Fig. 1A. As shown in Fig. 1A, the PCL enveloped the drugs to form a hydrophobic core, while the PEG extended outwards to form a hydrophilic shell in the aqueous phase. Meanwhile, the micelles exhibited a spherical structure and was no significant difference as observed by transmission electron microscopy (TEM) (Fig. 1B). The average diameter of micelles was 87.63 nm (Fig. 1C), and polydispersity index (PDI) was 0.189. The drug loading and encapsulation efficiency of AP were 10% and 97.4%, respectively. The drug loading and encapsulation efficiency of DOX were 5% and 90.3%, respectively. There was no significant change in micelle size at any time point in the pH 7.4 buffer. However, the micelles were unstable in the pH 5 buffer, leading to a rapid increase in micelle size with time. This could be attributed to the imine bond breaking under the influence of pH, which resulted in damage to the micelle structure (Fig. 1D).

Methylthiazolyldiphenyl-tetrazolium bromide (MTT) assay was used to investigate the cytotoxic effect of PEG-N-PCL@DOX, PEG-N-PCL@AP and PEG-N-PCL@Dox+AP in GL261 cell. Results showed almost no change in the PEG-N-PCL@AP group compared to the normal saline (NS) group, while the PEG-N-PCL@DOX, as well as the PEG-N-PCL@DOX + AP groups, showed significant changes. Af-

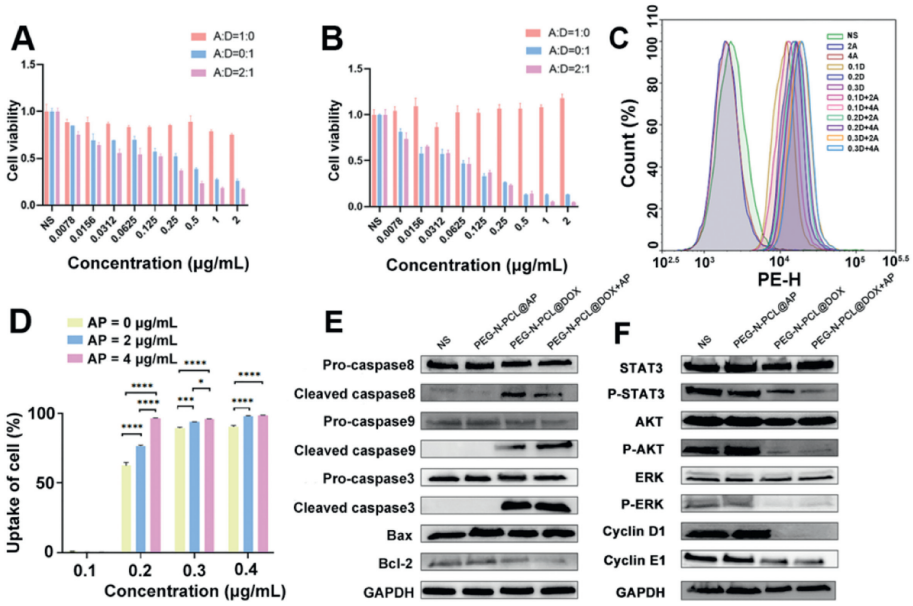

Fig. 2. *In vitro* anti-tumor effect of cRGD/PEG-N-PCL@DOX + AP in GL261 cells. (A, B) Cell cytotoxicity analysis. GL261 cell viability was measured by MTT assay after treatment with different concentrations of AP and DOX at 24 and 48 h. (C, D) Cell uptake statistics. (E) Western blot analysis of apoptosis protein expression in GL261 cells after treatment with different drugs. (F) Western blot analysis of proliferation and cell cycle protein expression in GL261 cells after treatment with different drugs. Data are presented as mean ± SD ($n = 3$). $^{*}P < 0.05$, $^{***}P < 0.001$, $^{****}P < 0.0001$. ERK, extracellular regulated protein kinase; GAPDH, glyceraldehyde-3-phosphate dehydrogenase.

ter incubation with drugs for 24 h, the cytotoxic effect of the PEG-N-PCL@DOX group and PEG-N-PCL@DOX + AP group was increasingly stronger compared with the NS group, and the killing effect was positively correlated with the drug concentrations ranging from 0.078 μg/mL to 2 μg/mL. When the concentration was equal to or more than 0.25 μg/mL, the killing effects on glioma cells of the PEG-N-PCL@DOX + AP group began to be more significant compared with the PEG-N-PCL@DOX group, with only 23.48% cell left at a concentration of 0.5 μg/mL (Fig. 2A). The results were measured after incubation with drugs for 48 h (Fig. 2B), and the PEG-N-PCL@AP group still did not change much compared with the NS group. As the duration of drug effects extended, the PEG-N-PCL@DOX + AP group and the PEG-N-PCL@DOX group exhibited more significant toxic effects on glioma cells after 48 h of drug treatment, and the trend of concentration inhibition was also more obvious. We also found that when the concentration was less than 1 μg/mL, there was little difference in the killing effect between the targeted and non-targeted groups. However, with the increase in drug concentration, the PEG-N-PCL@DOX + AP group still showed a superior tumor-killing effect than the PEG-N-PCL@DOX group. Identically, MTT assay was also used to determine the cytotoxic effect of those drugs on C6 cells after incubation for 24 and 48 h, and the results were similar to GL261 cell (Figs. S8A and B in Supporting information). Notably, when the concentration was in the range of 0.5–2 μg/mL, there was little difference in cell viability between the PEG-N-PCL@DOX + AP groups. Thus, in the follow-up work, we chose the concentration of 1 μg/mL DOX for the experimental study to exert a stronger tumor inhibitory effect with less dosage of DOX. In conclusion, AP might not have exerted a direct anti-tumor effect, but it might have enhanced DOX uptake and reversed chemoresistance. This is consistent with the fact that AP can enhance the inhibitory effect of chemotherapy such as docetaxel and DOX in multiple tumors [28,29]. Besides, AP can increase drug uptake to improve drug efficacy, which may improve the effective perfusion of tumor vessels and increase the intratumoral distribution of DOX in a certain time window *via* normalizing tumor vessels [30].

Meanwhile, prodium iodide (PI)/Annexin-V staining flow cytometry was used to detect the apoptosis of GL261 cells treated with AP or DOX monotherapy and their combinations. Compared with the control group, cells treated with DOX monotherapy demonstrated a significant increase in cell apoptosis in a dose-dependent manner. The apoptotic fractions of GL261 cells treated with 0.0625, 0.125, 0.25, 0.5 and 1 μg/mL DOX for 24 h were 8.35%, 9.72%, 11.43%, 20.58% and 66.06%, respectively (Figs. S9A and B in Supporting information). However, AP induced limited cell apoptosis following treatments, with only 1.87% apoptosis observed in 2 μg/mL at 24 h. In contrast, concomitant treatment of AP and DOX induced significantly higher level of cell apoptosis than either DOX or AP alone. The most prominent increase in apoptotic fractions was observed in cells treated with 0.5 μg/mL DOX + 1 μg/mL AP (72.52%) as compared with DOX alone (20.58%) and AP alone (1.53%). These findings suggested that AP could enhance the sensitivity of glioma to DOX. Similarly, DOX and AP demonstrated significant combined pro-apoptotic effects in C6 cells (Figs. S10A and B in Supporting information). Western blot assays were also conducted to identify potential apoptotic pathways involved in DOX/AP treatment. The cellular uptake of DOX was analyzed through flow cytometry (Figs. 2C and D, Fig. S11 in Supporting information). DOX alone could be taken up by GL261 cells, and the uptake was positively correlated with DOX concentration in a certain range. Notably, across all concentrations of DOX, the combination group consistently exhibited enhanced cell uptake rates compared to the DOX-alone group, with a more pronounced effect at lower DOX concentrations. Furthermore, AP significantly increased the intracellular uptake of DOX in GL261 cells in a dose-dependent manner. Similarly, the results of C6 cell uptake were coincident with those of GL261 cells (Figs. S12A–C in Supporting information). Therefore, the experimental result verified that the uptake rate of DOX by glioma cells could be significantly enhanced when combined with low-dose AP, thereby enhancing the anti-tumor effect and alleviating the adverse reactions caused by DOX treatment. Additionally, the reason for the increased uptake might be the suppression of drug efflux by AP. Several anti-angiogenic receptor tyrosine kinase inhibitors (TKIs), such as gefitinib, AP and sunitinib, were found to significantly inhibit major ATP-binding cassette transporter (ABC) transporters by interacting with or down-regulating their expression [31,32].

As shown in Fig. 2E and Fig. S13A (Supporting information), the apoptosis-related proteins, including caspase 8, caspase 9 and

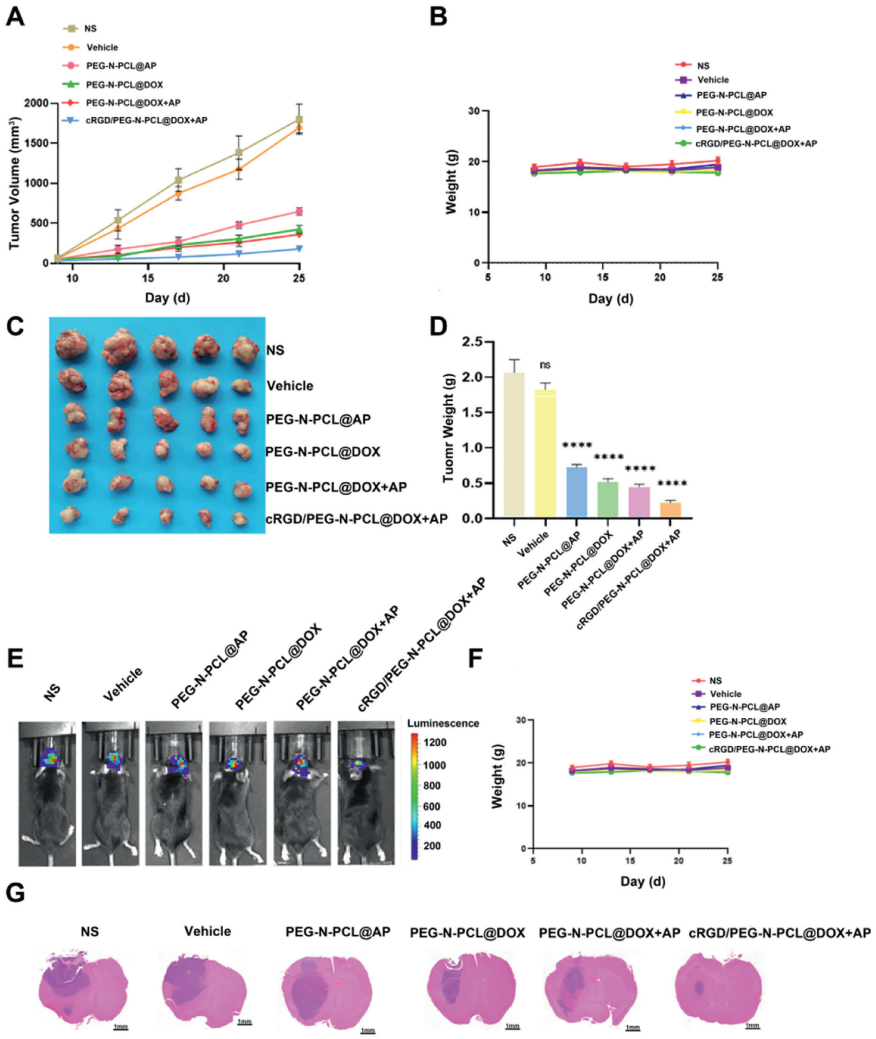

Fig. 3. Anti-tumor activity of cRGD/PEG-N-PCL@DOX + AP in a subcutaneous and orthotopic tumor model. (A) Trends in tumor volume in mice. (B) Trends in body weight of mice. (C) Pictures of mice tumors at the end of the experiment. (D) Schematic diagram of the tumor weight of mice at the end of the experiment. (E) Mouse intracranial tumor bioluminescence picture. (F) The body weight change curve of mice during treatment. (G) H&E staining images of intracranial tumors in each group of mice at the end of the 24-day treatment period. Scale bar: 1 mm. Data are presented as mean ± SD ($n = 5$). ns, $P > 0.05$; $^{****}P < 0.0001$ *vs.* the NS group.

caspase 3, were significantly activated in DOX and AP-treated glioma cells. Moreover, the anti-apoptotic protein Bcl-2 was downregulated and the pro-apoptotic protein Bax was upregulated in glioma cells following the combinational treatment of DOX and AP. These findings demonstrated that DOX and AP synergistically induced apoptosis of glioma cells through both intrinsic and extrinsic pathways.

In our quest to unravel the molecular underpinnings of the synergistic tumor suppression exerted by DOX and AP, we meticulously evaluated the status of three quintessential oncogenic pathways: the activator of transcription 3 (STAT3), protein kinase B (PKB or AKT), and the mitogen-activated protein kinase (MAPK) signaling cascades. Our in-depth analysis of GL261 cells post-treatment indicated that both DOX and AP, when applied separately, induced a reduction in phosphorylated STAT3 levels, with an even more pronounced effect observed upon concurrent administration. This attenuation in STAT3 activation was specific to its phosphorylation, as the overall expression level of STAT3 remained unchanged, highlighting a targeted suppression of STAT3 activity by the combined therapy. Moreover, the concomitant DOX and AP treatment was found to decrease the levels of phosphorylated MAPK and AKT, without any concomitant changes in the total protein levels of these kinases. This selective modulation of key oncogenic pathways is posited to be central to the enhanced anti-tumor efficacy observed with the DOX and AP combination. The treatment also notably curbed the expression of critical cycle-related proteins, such as cyclin D1 and cyclin E1, as depicted in Fig. 2F. A parallel downregulation of STAT3 and AKT pathways was observed in C6 cells, as shown in Fig. S13B (Supporting information).

In vivo validation of our *in vitro* findings was pursued through the establishment of a subcutaneous glioma mouse model. The tumor-bearing mice were subjected to a regimen of intravenous treatments with either NS, vehicle, PEG-N-PCL@DOX, PEG-N-PCL@AP, PEG-N-PCL@DOX + AP, or cRGD/PEG-N-PCL@DOX + AP, administered at two-day intervals, with tumor volume and weight monitored every four days. The data presented in Figs. 3A–D, revealed that the mice in the targeted combination therapy group exhibited the smallest average tumor volume and weight, in stark contrast to the other groups. The DOX and AP combination significantly impeded tumor progression compared to monotherapy, corroborating our *in vitro* results. Notably, no significant alterations in body weight were observed across all treatment groups throughout the study period, as shown in Fig. 3B. Safety assessments, encompassing both histological examination of vital organs and blood

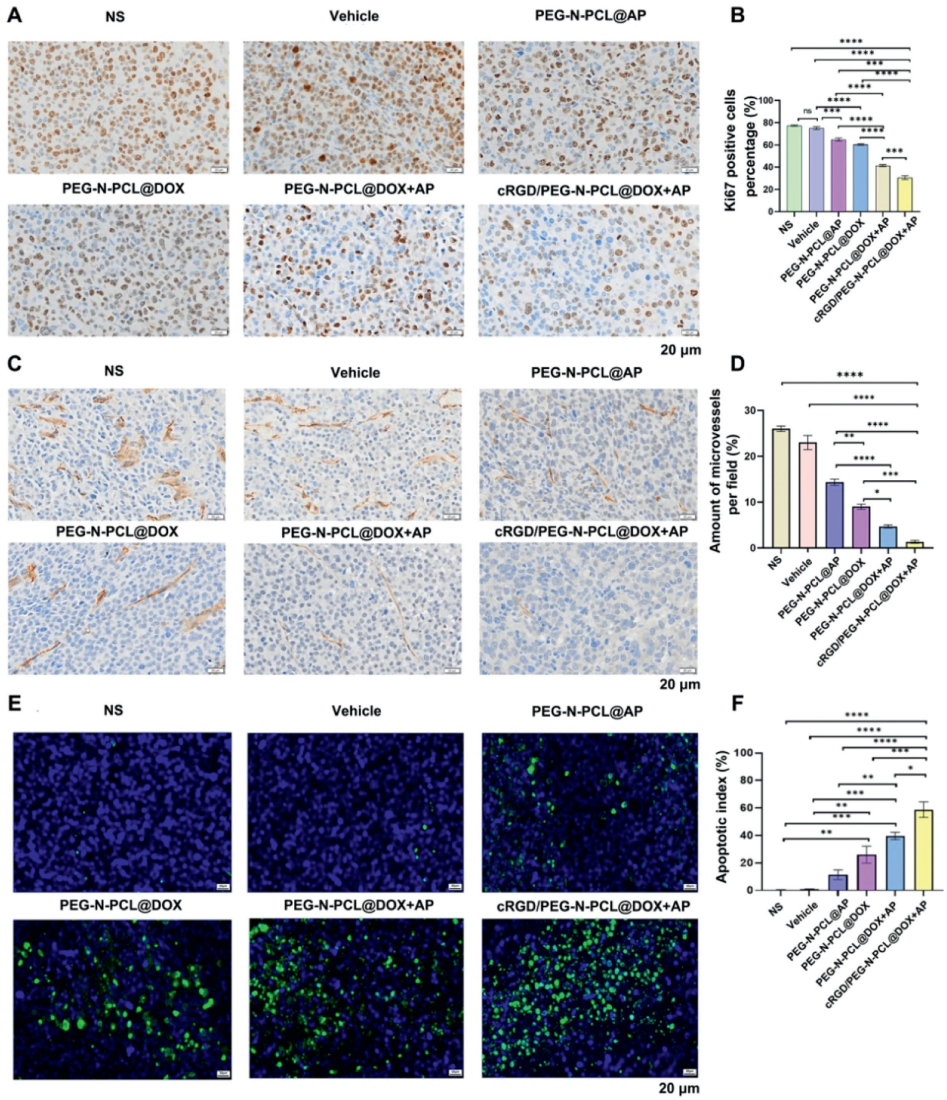

Fig. 4. cRGD/PEG-N-PCL@DOX + AP enhanced the inhibition of cell proliferation and angiogenesis, and the induction of apoptosis in the GL261 subcutaneous tumor. (A) Representative Ki67 staining images of tumors from different therapeutic groups. (B) Statistical analysis of Ki67-positive cells. (C) Representative CD31 staining images of tumors from different therapeutic groups. (D) Statistical analysis of microvessels. (E) Representative TUNEL staining images of tumors from different therapeutic groups (blue: cell nuclei; green: apoptosis cells). (F) Statistical analysis of apoptosis cells. Data are presented as mean ± SD ($n = 5$). $^{*}P < 0.05$, $^{**}P < 0.01$, $^{***}P < 0.001$, $^{****}P < 0.0001$. One-way ANOVA testing. Scale bar: 20 μm.

biochemical analyses, indicated no significant treatment-related adverse effects, as detailed in Figs. S14 and S15 (Supporting information). These findings collectively suggested that the co-delivery of DOX and AP using cRGD-modified micelles could be a highly effective strategy for glioma suppression, with a significant therapeutic impact and an acceptable safety profile.

We further constructed an orthotopic GL261 glioma mouse model to verify the anti-glioma effect of the system. The tumor-bearing mice were intravenously treated with NS, vehicle, PEG-N-PCL@DOX, PEG-N-PCL@AP, PEG-N-PCL@DOX + AP, and cRGD/PEG-N-PCL@DOX + AP every two days for 4 times. According to fluorescence intensity, although a single treatment with DOX and AP both induced substantial tumor shrinkage in the brain, and the free drug combination group showed better efficacy, the group treated with DOX/AP-loaded PCL-PEG-cRGD was the most effective in diminishing tumor size (Fig. 3E). Additionally, there was no significant change in body weight during the treatment (Fig. 3F). Furthermore, it was evident that the DOX/AP-loaded PCL-PEG-cRGD group exhibited the smallest tumor volume in brain tissues, as indicated by hematoxylin and eosin (H&E) staining (Fig. 3G).

Immunohistochemical analyses of tumor tissues were also performed to evaluate tumor cells proliferation *in vivo*, characterized by the expression of Ki67 and CD31. After treating with PEG-N-PCL@DOX, PEG-N-PCL@AP, PEG-N-PCL@DOX + AP and cRGD/PEG-N-PCL@DOX + AP, the Ki67 index was significantly decreased. Notably, the combination treatment showed a greater effect than monotherapy. The PEG-N-PCL@DOX + AP group had the lowest Ki67 index among the treatment groups (Figs. 4A and B). Likewise, the tumors treated with DOX/AP-loaded PCL-PEG-cRGD showed the lowest CD31 expression level (Figs. 4C and D). These results collectively suggested the inhibitory effect of DOX/AP-loaded PCL-PEG-cRGD on cells proliferation and neovascularization of GL261 glioma *in vivo*. Furthermore, we evaluated the apoptosis of the subcutaneous GL261 model by TdT-mediated dUTP nick-end labeling (TUNEL) staining. When compared with the single use of DOX and AP or non-targeted combination therapy, the DOX/AP-loaded PCL-PEG-cRGD group showed more signals, which indicated the apoptosis of cells (Figs. 4E and F). Hence, it was demonstrated that the combination therapy by cRGD-modified nanoparticles significantly improved anti-tumor activity by inducing cells apoptosis.

All animal experiments were approved by the Animal Experimental Ethics Committee of the State Key Laboratory of Biotherapy (SKLB) of Sichuan University.

In conclusion, we have confirmed that the combined treatment of glioma with DOX and AP could achieve better therapeutic efficacy. Additionally, the application of pH-responsive PCL-PEG-cRGD nanoparticles could further improve the therapeutic efficacy while maintaining favorable safety. Therefore, DOX/AP-loaded pH-sensitive PCL-PEG-cRGD is a promising therapeutic candidate for the treatment of glioma.

Declaration of competing interest

The authors declare that they have no known competing financial interests or personal relationships that could have appeared to influence the work reported in this paper.

CRediT authorship contribution statement

Hongyi Huang: Writing – original draft, Methodology. **Siyao Che:** Resources, Investigation. **Wenjie Zhou:** Methodology, Formal analysis. **Yunchu Zhang:** Project administration. **Weiling Zhuo:** Project administration. **Xijing Yang:** Supervision, Software. **Songping Zheng:** Funding acquisition. **Jiagang Liu:** Writing – review & editing, Funding acquisition. **Xiang Gao:** Writing – review & editing, Writing – original draft, Funding acquisition.

Acknowledgments

This work was supported by Sichuan Science and Technology Program, China (No. 2023YFS0273), and the 1·3·5 Project for Disciplines of Excellence, West China Hospital, Sichuan University, China (No. ZYJC21022).

Supplementary materials

Supplementary material associated with this article can be found, in the online version, at doi:10.1016/j.cclet.2024.110084.

References

[1] Q.T. Ostrom, H. Gittleman, G. Truitt, et al., Neuro. Oncol. 20 (2018) iv1–iv86.
[2] L.R. Schaff, I.K. Mellinghoff, JAMA 329 (2023) 574–587.
[3] R.K. Oberoi, K.E. Parrish, T.T. Sio, et al., Neuro. Oncol. 18 (2016) 27–36.
[4] J. Liu, Z. Zhao, N. Qiu, et al., Nat. Commun. 12 (2021) 2425.
[5] C. Wang, R. Zhang, J. He, et al., Nat. Commun. 14 (2023) 3877.
[6] H. Chen, S. Zhang, Q. Fang, et al., ACS Nano 17 (2023) 421–436.
[7] H.P. Hu, L.J. Yu, Z. Ding, et al., Chin. Chem. Lett. 34 (2023) 108592.
[8] C.C. Xue, M.H. Li, Y. Zhao, et al., Sci. Adv. 6 (2020) eaax1346.
[9] J.A. Pan, H. Zhang, H. Lin, et al., Redox. Biol. 46 (2021) 102120.
[10] K.T. Sawicki, V. Sala, L. Prever, et al., Annu. Rev. Pharmacol. Toxicol. 61 (2021) 309–332.
[11] R.S. Apte, D.S. Chen, N. Ferrara, Cell 176 (2019) 1248–1264.
[12] H. Seyedmirzaei, P. Shobeiri, M. Turgut, et al., Rev. Neurosci. 32 (2021) 191–202.
[13] Y.J. Mi, Y.J. Liang, H.B. Huang, et al., Cancer Res. 70 (2010) 7981–7991.
[14] W.T. Ju, R.H. Xia, D.W. Zhu, et al., Nat. Commun. 13 (2022) 5378.
[15] H. Lin, X.L. Zhou, X.F. Sheng, et al., Drug R D 23 (2023) 239–244.
[16] H. Yao, J. Liu, C. Zhang, et al., Cell. Death. Dis. 12 (2021) 927.
[17] X.X. Liu, C.X. Zheng, Y.Y. Kong, et al., Chin. Chem. Lett. 33 (2022) 328–333.
[18] M.T. Manzari, Y. Shamay, H. Kiguchi, et al., Nat. Rev. Mater. 6 (2021) 351–370.
[19] H. Liu, Z.H. Miao, Z.B. Zha, Chin. Chem. Lett. 33 (2022) 1673–1680.
[20] C.Y. Liu, J.H. Lan, Q.B. Yan, et al., Chin. Chem. Lett. 33 (2022) 3561–3564.
[21] P.J. Hanwright, C. Qiu, J. Rath, et al., Biomaterials 280 (2022) 121244.
[22] R.X. Han, Q.Y. Liu, Y. Lu, et al., Biomaterials 281 (2022) 121328.
[23] K.Y. Wang, Y.A. Xiang, W. Pan, et al., Chin. Chem. Lett. 33 (2022) 793–797.
[24] Y. Zou, J. Wei, Y. Xia, et al., Signal. Transduct. Target. Ther. 3 (2018) 32.
[25] M.C. Robitaille, J.A. Christodoulides, J. Liu, et al., ACS Appl. Mater. Interfaces 12 (2020) 19337–19344.
[26] X.B. Chen, H. Yang, X. Song, et al., Chin. Chem. Lett. 34 (2023) 107753.
[27] Y.Z. Sun, L.D. Gong, Y. Yin, et al., Adv. Mater. 34 (2022) e210958.
[28] S.Q. Feng, G.J. Wang, J.W. Zhang, et al., Acta Pharmacol. Sin. 39 (2018) 1670–1680.
[29] Y. He, X. Li, J. Ma, et al., Small 15 (2019) e1804397.
[30] K. Zhou, J.W. Zhang, Q.Z. Wang, et al., Acta Pharmacol. Sin. 40 (2019) 556–562.
[31] G.L. Beretta, G. Cassinelli, M. Pennati, et al., Eur. J. Med. Chem. 142 (2017) 271–289.
[32] X.L. Li, Y. He, J.W. Hou, et al., Small 16 (2020) 1902262.